# Comparison of Quasi-Simultaneous Outdoor-to-Indoor Propagation Loss and Delay Dispersion Measurements at 150, 450, and 700 MHz

R. Bultitude, T. Smith, D. Cule, and H.Zhu
Radio Propagation Research Division
Communications Research Centre
Ottawa, Canada
robert.bultitude@crc.ca, tyler.smith@crc.ca, dino.cule@crc.ca

***Abstract*—This paper reports wideband propagation measurements that were conducted to compare characteristics on outdoor-to-indoor radio links in the 150 MHz, 450 MHz, and 700 MHz frequency bands. Propagation losses, excess losses with respect to free space loss, and delay dispersion values are compared.**

***Keywords-Propagation Loss, Delay dispersion, multipath propagation, building penetration***

## I. INTRODUCTION

Following the re-farming of spectrum in the 700 MHz band, some existing users of the 150 MHz and 450 MHz bands have been encouraged to consider the extension of their systems through migration to the 700 MHz band. Additionally, public safety organisations are considering the design of new emergency systems for operation in this band. To aid in the design of new systems in the 700 MHz band, this paper reports wideband outdoor-to-indoor propagation measurements that were made at the Communications Research Centre (CRC) in Ottawa, for the estimation and comparison of propagation characteristics in the three aforementioned bands. Section II describes the measurement equipment and data processing. Section III reports on the propagation scenario where the measurements were made. Section IV shows results, and conclusions can be found in Section V.

## II. MEASUREMENT EQUIPMENT AND DATA PROCESSING

It is well-known that multipath propagation results in spatial variations of received powers over small local areas. For this reason, propagation loss is usually characterised by averaging measurements made over (small) local areas, often using an antenna on a rotating arm. However, because of space limitations and antenna considerations associated with the desire to make quasi-simultaneous measurements in the three bands of interest, the rotation of antenna(s) for spatial averaging was considered impractical. Instead, experiments were designed to allow averaging over large bandwidths in place of spatial averaging. A channel sounder was therefore designed using mostly existing transmitter (Tx) and receiver (Rx) subsections to transmit 50 Mchps pseudonoise (PN) sounding signals centred on 150 MHz, 450 MHz, and 700 MHz. It should be noted that, in the lower two frequency bands, the system qualifies as a UWB system.

At the Tx, an FPGN-generated 255-chip, 50 Mchps PN sequence is split, appropriately buffered, and applied to 3 pre-existing complex modulator circuits for BPSK modulation on a 330 MHz carrier, followed by upconversion to 2.25 GHz. The three identical, modulated, 2.25 GHz output signals were then bandpass filtered to 2.25 GHz +/- 50 MHz, and each was downconverted to one of the three frequency bands of interest, bandpass filtered with 100 MHz bandwidth, and amplified, such that a maximum transmit power of +36 dBm could be achieved in each band. The Tx output signals were then fed through variable attenuators and a triplexer to a DRDC Model Bic130A very wideband biconical antenna[1].

The Rx was designed for mounting in a motorised equipment rack that can be moved throughout a building using WiFi remote control. Signals received by an identical biconical antenna to that used at the Tx are first applied to one of three selectable bandpass filters, with each centred on one of the bands of interest, then to a wideband LNA, and subsequently to a wideband frequency mixer, the LO signal input to which is selected simultaneously with the input bandpass filter, so as to generate an LO signal appropriate for upconversion of the received signal to 2.25 GHz. The upconverted 2.25 GHz is then bandpass filtered to 2.25 GHz +/- 100 MHz, amplified, and applied to a ThinkRF Inc. WSA2250 wireless spectrum analyzer (WSA). The WSA performs a single downconversion to complex baseband, and, after receiving an appropriate trigger signal, samples each of the in-phase and quadrature outputs from the downconverter at 100 MSamples/s. Inputs to the WSA include the received

[1] Such antennas are available from Defense Research and Development Canada, in Ottawa, and cover a frequency range between 100 MHz and 6 GHz, with an omnidirectional H plane radiation pattern over the complete frequency range.

978-1-4673-1881-5/12/$31.00 ©2012 IEEE

signal, a 2.25 GHz sinewave downconversion LO signal from a PLO, a 100 MHz sinewave used as the sample clock, and a trigger signal to enable the recording of data snapshots at a rate of 20 snapshots/s. All reference, oscillator, and trigger sources in the measurement system are slaved to Rb frequency standards, conditioned using signals received from the global positioning satellite system.

Each data snapshot recorded by the WSA contains 4000 complex samples, 1/3 of which were recorded while the Rx front-end filters and upconverter LO were chosen so as to select one of the 3 bands of interest. One sequence length (510 samples) of the data recorded in each data snapshot from the received signal in each frequency band is selected for later processing.

Processing each data snapshot of field measurements involved cross correlation of the signal received in each band with the signal received in each band through the system when the Tx was connected back-to-back (BB) to the Rx through a coaxial cable and attenuator used to simulate an ideal channel. This is equivalent to cross correlating the output from the radio channel with its input, which, in the case of a pseudo-noise channel sounding signal, yields a good estimate of the impulse response of the radio channel, modelled as a linear filter [1]. Impulse response estimates (IREs) so-derived were thresholded [2], so that only 1 sample of noise in each 511 samples could be mistaken as being a multipath signal contribution, then their squared magnitudes were summed to estimate uncalibrated Rx output signal powers. Such powers were then compared against system output powers that were recorded under BB connections with known input powers from the transmitter to estimate absolute received signal powers. The system was calibrated so as to linearly respond to received signal powers between -30 dBm and -77 dBm in the 150 MHz, band, between -30 dBm and -90 dBm in the 450 MHz band, and between -30 dBm and -92 dBm in the 700 MHz band.[2] Accuracy of propagation loss results was verified through identical BB and off-air signal power measurements using the channel sounder and using an Agilent E4448A Spectrum Analyser.

## III. Propagation Scenario

The Tx/Rx configuration used during the measurements is depicted in Fig. 1. The figure shows the footprint of the

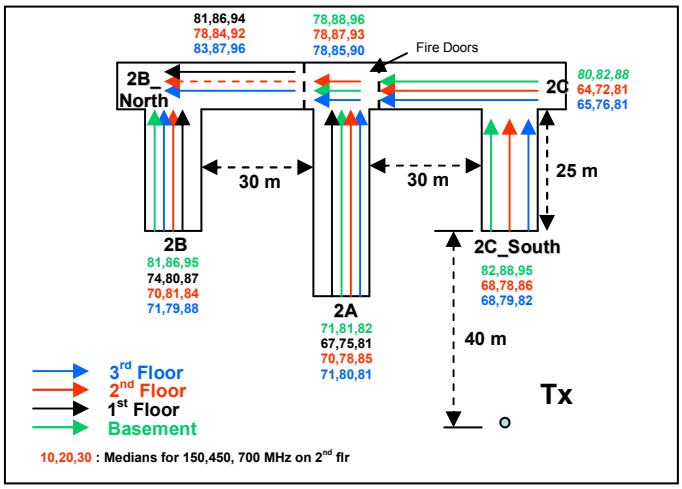


Fig. 1. Plan view of the propagation measurement scenario.

1950s style brick building. Coloured arrows indicate the trajectory of the receive trolly on each of the four floors, whereas the similarly-coloured numbers indicate median measured propagation losses, and will be discussed later.

The measurement system Tx was installed at the channel sounder base station (CSBS), which was housed in a trailer parked 40 m from the nearest wing of the building. Its biconical antenna was raised from the trailer roof to a height of 4 m above ground level. Maximum power delivered to the antenna feedpoint was +36 dBm in each frequency band The system Rx was installed in the motorised equipment rack (trolly), and it, along with the laptop computer used for remote control and data recording, formed the channel sounder mobile station (CSMS). A photograph of the CSMS during a run on the second floor hallway in Blg 2A is shown in Fig. 2.

Fig. 2. Photograph of the remotely controlled CSMS moving along the 2nd floor hallway in Bldg 2A with its biconical Rx antenna.

## IV. Results

### A. Time Series Data from Single Measurement Runs

Fig. 3 shows propagation loss data from the 2nd floor hallway of Bldg 2A shown in Fig. 2. This time series is

[2] Differences in these ranges were associated with differences in impedance matching and gains in the wideband receiver front end.

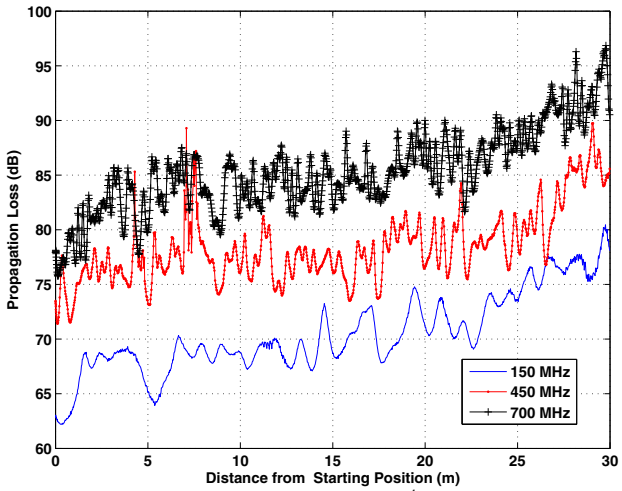

Fig. 3 Propagation loss time series from the 2nd floor of Bldg. 2A.

typical, and clearly shows that mean propagation loss increases as operating frequency increases. It can also be seen that there are still spatial variations of received power about a spatially-varying mean, despite the 100 MHz bandwidth. These variations are small, however (5 dB pk-pk), and they are roughly centred on the means, so it is considered reasonable to conclude that their influence on medians, are insignificant. Thus, no further averaging was applied to derive propagation loss results reported in the following. It is also noteworthy that the CSMS trajectory was directed away from the outdoor CSBS Tx, so the increase in propagation loss with distance is as would be expected.[3]

Fig. 4 shows a time series measured along one of the basement trajectories where propagation losses exhibited unexpected behaviour, the propagation loss at 700 MHz being almost the same as that at 450 MHz.

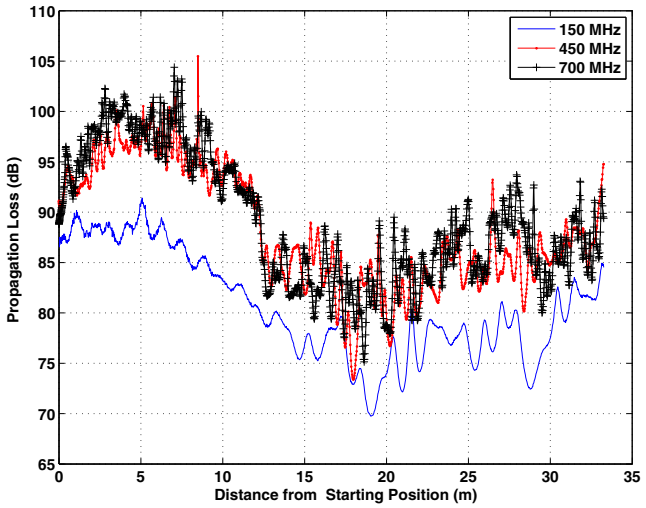

Fig. 4 Time series of propagation loss results from along the basement hallway in Bldg. 2C.

[3] Note that the distance plotted is respect to the starting point on the CSMS trajectory, not the distance from the Tx.

Results from four other runs showed unexpected behaviour. In three cases, the propagation loss at 700 MHz over significant portions of the trajectories (3rd floor, Bldg 2A, Basement, Bldg 2A and 2nd floor, Bldg 2B) was approximately equal to, or only slightly greater than the propagation loss at 450 MHz, and lower than is typical. In the remaining case, over a 3rd of the trajectory on the first floor of Bldg 2B, propagation loss at 450 MHz was approximately equal to the propagation loss at 150 MHz, and lower than is typical.

### *B. Overall Propagation Loss Statistics*

To derive overall conclusions, propagation loss values from single-snapshot measurements in all three bands were taken as triplets for the estimation of the probability that loss is greater in a specified band than in another, and of a complimentary cumulative probability distribution function (CCDF) for propagation loss in each band. A total of 23,661[4] propagation loss triplets were used to obtain these estimates. Table 1 shows the probability of loss in a specified band being greater than that in another. It is clear from the table that, on a statistical basis, anomalies wherein propagation loss is lower in a higher frequency band are rare. The CCDFs for propagation loss are shown in Fig. 5. This figure shows that the probability that a specific propagation loss value is exceeded is greater at 700 MHz. The median in this band is 13 dB greater than the median at 150 MHz, and the median at 450 MHz is 7 dB greater than the median at 150 MHz.

**Table 1. Probabilities for Specified Loss Comparisons, Based on 26,661 Data Values Measured at CRC**

| Probability | Value of Specified Probability |
|---|---|
| Prob[L700<L150] | 98% |
| Prob[L700<L450] | 92% |
| | |
| Prob[L450<L150] | 93% |
| | |

The small coloured numbers printed on Fig. 1 near the arrows that represent measurement runs are the medians at 150 MHz, 450 MHz, and 700 MHz, respectively (in this sequence) of propagation loss values estimated for that run. If these values are compiled, their medians are as shown in Table 2. These results show that the median losses from an outside Tx to a basement receiver are 6-8 dB greater in all 3 bands than the median propagation loss to a receiver on the 1st floor. Median propagation losses at 150 MHz and 700 MHz were

[4] It is expected that there was significant correlation among consecutively measured data since the CSMS moved slowly. However, because of the large number of measurements over a large area, it is believed that error bounds on these estimates are fairly tight.

slightly less on the upper two floors, which were closer to the elevation of the CSBS Tx antenna than the first floor.

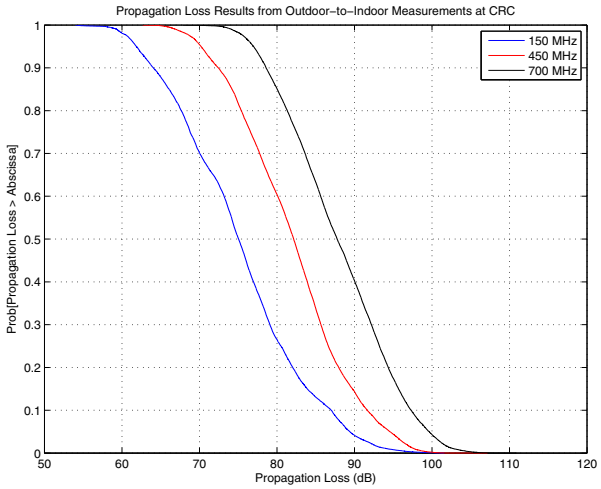


Fig. 5 CCDFs for outdoor-to-indoor propagation measured in Bldg 2 at CRC.

**Table 2. Medians of the Results in Fig. 1**

| | Median Propagation Loss (dB) | | |
|---|---|---|---|
| **Frequency band** | **150 MHz** | **450 MHz** | **700 MHz** |
| **Basement** | 80 | 86 | 95 |
| **1st floor** | 74 | 80 | 87 |
| **2nd floor** | 70 | 80 | 86 |
| **3rd floor** | 71 | 80 | 85 |

### *C. Excess transmission and Building Penetration Losses*

Knowledge of the distance between the CSBS Tx and the starting points of all measurement runs, coupled with knowledge of distance travelled by the CSMS was used to calculate free space losses for every measurement run. The difference between these and measured losses are termed "excess losses" herein, and are given in Table 3. An associated CCDF can be seen in Fig. 6. Note that fewer data (10,800 values) were used to compile these results than others reported herein because data from inner portions of the building for which propagation paths may have been very complicated were not considered. It can be seen from both the Table and the CCDF that excess losses, as well as the probability of exceeding specified values, were greater in the 700 MHz band. Other trends in the table are the same as those discussed in foregoing paragraphs in relation to absolute propagation losses. For a few cases, such as in Bldg C and Bldg 2 A, received signals would have most likely propagated directly through a single building skirt wall, and reported values likely are good estimates of building penetration loss. Of particular interest are the results for the 2nd and 3rd floors of these two buildings, where it can be seen that such values were between 6 and 7 dB greater for Bldg 2A. It is believed that this is a result of the fact than the angle of incidence upon the face of Bldg 2A was significantly greater than that upon the face of Bldg 2C.

**Table 3. Excess Propagation Losses**

| **Bldg** | | **150 MHz** | **450 MHz** | **700 MHz** |
|---|---|---|---|---|
| **2A** | **Bmt** | 31 | 26 | 26 |
| | **1st** | 21 | 21 | 25 |
| | **2nd** | 22.3 | 22.6 | 29 |
| | **3rd** | 25 | 26 | 31 |
| **2B** | **Bmt** | 21 | 18 | 26 |
| | **1st** | 23 | 22 | 27 |
| | **2nd** | 19 | 23 | 24 |
| | **3rd** | 21 | 20 | 28 |
| **2B_North** | **Bmt** | - - | - - | - - |
| | **1st** | 32 | 31 | 36 |
| | **2nd** | 28 | 26 | 33 |
| | **3rd** | 33 | 30 | 36 |
| **2C** | **Bmt** | 31 | 30 | 30 |
| | **1st** | - - | - - | -- |
| | **2nd** | 15.2 | 15.6 | 23 |
| | **3rd** | 16 | 19 | 23 |
| **2C_South** | **Bmt** | 38 | 36 | 42 |
| | **1st** | - - | - - | - - |
| | **2nd** | 24 | 25 | 32 |
| | **3rd** | 24 | 28 | 29 |

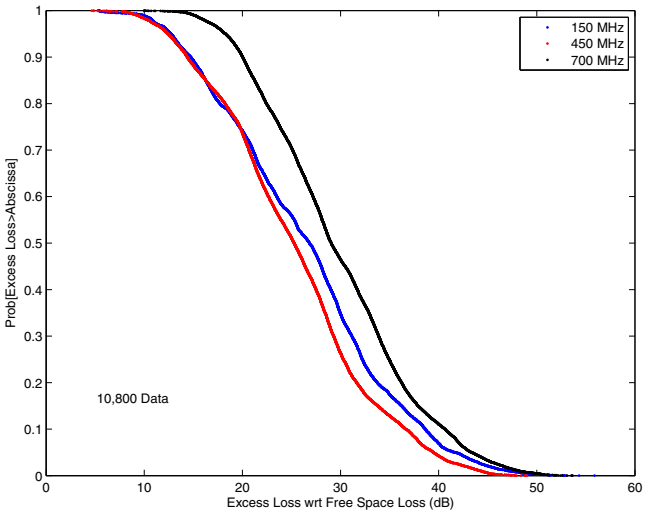


Fig. 6. CCDF for excess loss in Bldg 2 at CRC.

### *D. Delay Dispersion*

Available also from the measured data is information concerning delay dispersion. The measured time series have the characteristics of non stationary random processes. It is therefore difficult to obtain estimates of averages having small standard errors from them, and this task will be left for later work. Rms delay spreads estimated from average power delay profiles, which can be used for the assessment of error rates, for example, cannot be reported. However, it is possible to report the power-weighted standard deviations of multipath

component delays from single impulse response estimates. Such are referred to herein as to as static rms delay spreads, and they are computed using the same equations that are used to estimate rms delay spreads, except that they are applied to data from single snapshots, rather than to averages. They are useful for a quantitative assessment and comparisons of delay dispersion on different radio links, or on the same radio links, but in different frequency bands. In this paper, such results were compared for the same pool of data as that used for the comparison of propagation losses. As for the propagation losses, after noise rejection thresholding, triplets of static rms delay spread data were assembled from each of 23,548 data[5] snapshots. Resulting CCDFs for static rms delay spread are shown in Fig. 7.

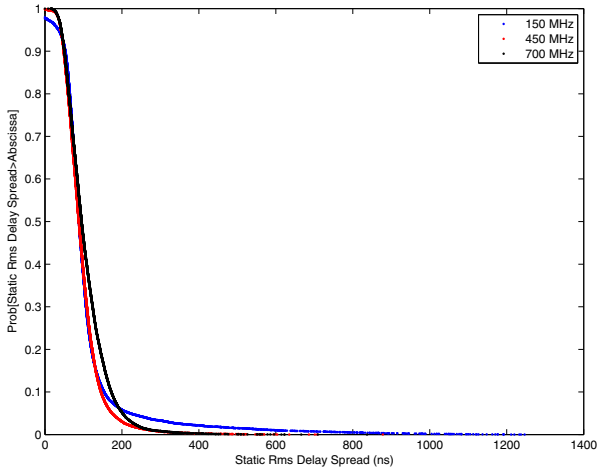


Fig. 7 CCDF for Static Rms Delay Spreads, estimated from all data measured in Bldg 2 at CRC.

The medians in Fig. 6 are 88, 88, and 95 ns at 150 MHz, 450 MHz and 700 MHZ, respectively. It can be seen clearly below the medians that there is greater probability that static rms delay spreads are greater than any specified value at 700 MHz up to values of about 190 ns, and thereafter, the probability of this occurring at 150 MHz is greater. The probability of very large static rms delay spreads, up to and greater than 1200 ns is almost zero at 450 MHz and 700 MHz, whereas it is nonzero at 150 MHz. The reason for this is believed to be the greater effective aperture of the biconical antennas at 150 MHz. This would, of course be true for any resonant antenna, and leads to an often quoted lower free space loss for radiowaves with lower frequencies. It is believed that the greater probability of exceeding a particular static rms delay spread at 700 MHz, for values less than 190 ns could be a result of the fact that there are a greater number of objects (e.g. furniture) that are large enough to generate good specular reflections at 700 MHz than there are in the lower frequency bands.

[5] The number of data used to compile the propagation loss and delay dispersion CCDFs is slightly different because of the exclusion of outliers peculiar to each of the two cases.

While the CCDFs in Fig. 7 give overall statistics, it is also of interest to know the probability that static rms delay spread is greater in one band than in another at any particular location. This can be estimated from the triplets of values for each data snapshot, and results are reported in Table 4. These

**Table 4. Probabilities for Specified Static Rms Delay Spread Comparisons, Based on 23,548 Data Values Measured at CRC**

| Probability | Value of Specified Probability |
|---|---|
| Prob[DS_static700<DS_static150] | 48% |
| Prob[DS_static700<DS_static450] | 41% |
| | |
| Prob[DS_static450<DS_static150] | 54% |

values are fairly close to 50%, but as for the CCDFs in Fig.7, the tendency for static rms delay spreads to be greater at 700 MHz is apparent.

## V. CONCLUSIONS

Results reported herein show that absolute, as well as excess outdoor-to-indoor propagation losses are greater in the 700 MHz band than they are in the 150 MHz and 450 MHz bands, although anomalous results can occur in some indoor locations, particularly in basements. A tendency for slightly greater static rms delay spreads exists also in the 700 MHz band, for values up to about 190 ns. There is a greater probability, however , for greater static rms delay spreads than this at 150 MHz. At any given measurement location, the probability that rms delay spread in one of the 3 bands is greater than that in another band is about 50%.

## ACKNOWLEDGEMENT

The authors would like to acknowledge the support of Drs. Yvo de jong and Georgy Levin in the design and programming of switch timing circuitry for the receiver front end, and software for control of the remotely controlled receiver dolly. Unfortunately neither could be available for the field work or data analysis.

## References

[1] R.W. Hubbard, R.F. Linfield, and W . J . Hartman, “Measuring characteristics of microwave mobile channels,” Proc., IEEE Vehicular Technology Conf., Denver, March 22-24, 1978, pp. 519-526.

[2] E.S. Sousa, V.M. Jovanovic, and C. Daignault, “Delay spread measurements for the digital cellular channel in Toronto,”IEEE Trans., veh. Technol.,vol.. 33, no. 4., Nov. 1974, pp.837-847.